FORWARD AND INVERSE KINEMATICS ANALYSIS AND VALIDATION OF THE ABB IRB 140 INDUSTRIAL ROBOT

Mohammed Almaged[1*], Omar Ismael[2]
[1,2] Nineveh University, College of Electronics Engineering,
Department of Systems & Control Engineering, Nineveh, Iraq

ABSTRACT

The main goal of this paper is to derive the forward and inverse kinematics model of the ABB IRB 140 industrial manipulator. This work provides essential kinematics information that could be a useful reference for future research on the robot. It can also serve as teaching material for students in the area of robotics, especially forward and inverse kinematics, to aid students' understanding of these subjects. Denavit-Hartenberg analysis (DH) is presented to write the forward kinematic equations. Initially, a coordinate system is attached to each of the six links of the manipulator. Then, the corresponding four link parameters are determined for each link to construct the six transformation matrices (${}_{i}^{i-1}T$) that define each frame relative to the previous one. While, to develop the kinematics that calculates the required joint angles ($\theta_1 - \theta_6$), both geometrical and analytical approaches are used to solve the inverse kinematic problem. After introducing the forward and inverse kinematic models, a MATLAB code is written to obtain the solutions of these models. Then, the forward kinematics is validated by examining a set of known positions of the robot arm, while the inverse kinematics is checked by comparing the results obtained in MATLAB with a simulation in Robot Studio.

KEYWORDS: *Robotics; Forward Kinematics; Inverse Kinematics; IRB 140 Manipulator*

1.0 INTRODUCTION

'Kinematics is the science of geometry in motion' (Jazar, 2010). This means it deals only with geometrical issues of motion such as the position and orientation regardless the force that causes them. There are two types of kinematics, the forward and inverse kinematics. Forward kinematic analysis is concerned with the relationship between the joint angle of the robot manipulator and the position and orientation of the end-effector (Spong, Hutchinson, & Vidyasagar, 2006) (Paul, 1981) . In other words, it deals with finding the homogeneous transformation matrix that describes the position and orientation of the tool frame with respect to the global reference frame. On the other hand, inverse kinematics is used to calculate the joint angles required to achieve the desired position and orientation. The same transformation matrix which resulted from the forward kinematics in order to describe the position and the orientation of the tool frame relative to the robot base frame is used here in the inverse kinematics to solve for the joint angles. Several academic studies investigating the kinematics of the robot manipulators have been carried out to increase their intelligence and usability. Various

*Corresponding author e-mail: m_engineer89@yahoo.com

approaches have been introduced for the analysis. In his book, Selig (Selig, 2013) has discussed several ways of analyzing robots using geometrical approach. Jazar (Jazar, 2010) also reviewed a number of analytical methods for the analysis of serial robots. The concept of the homogeneous transformation matrix is very old in the area of kinematic analysis. However, it is still very popular and valuable.

Several authors (Craig, 2005; Jazar, 2010; Shahinpoor, 1987; Uicker, Pennock, & Shigley, 2011) have discussed the formulation of the homogeneous transformation matrix. In 2012, K. Mitra introduced a different procedure for the formulation of the homogeneous matrix. His method was based on motion transfer at the joints from the base to the end effector. This technique was validated through a numerical study on a 5 DOF robot (Mitra, 2012). Also, A. Khatamian produced a new analytical method for solving the forward kinematics of a six DOF manipulator (Khatamian, 2015).

Several approaches have been used to solve the inverse kinematic problem. Some researchers have investigated the inverse kinematics of robot manipulators using standard techniques such as geometric, algebraic, etc. In 2012, Deshpande and George presented an analytical solution for the inverse kinematics derived from the D-H homogeneous transformation matrix (Deshpande & George, 2012). In the same vein, Neppalli et al developed a closed-form analytical approach to solve the inverse kinematics for multi-section robots. In this novel approach, the problem is decomposed into several easier sub-problems. Then, an algorithm is employed to produce a complete solution to the inverse kinematic problem (Neppalli, Csencsits, Jones, & Walker, 2009). S. Yahya et al proposed a new geometrical method to find the inverse kinematics of the planar manipulators (Samer Y, 2009).

Other researchers have solved the inverse kinematic problem using advanced techniques such as artificial neural network and biomimetic approach. In 2014, Feng et al produced a novel learning algorithm, called extreme learning machine, based on a neural network to generate the inverse kinematic solution of robot manipulator (Feng, Yao-nan, & Yi-min, 2014). The findings of this advanced method revealed that the extreme learning machine has not only significantly reduced the computation time but also enhanced the precision.

2.0 ROBOT SPECIFICATIONS

Figure 1 shows the compact six degree of freedom industrial ABB IRB 140 manipulator. The robot has six revolute joints controlled by Ac-motors. It is designed specifically for manufacturing industries to perform a wide range of applications such as welding, packing, assembly, etc. The specifications, axes and dimensions of the robot manipulator are shown below in Table 1.

Table 1. The ABB IRB 140 specifications (ABB, 2000)

Manipulator Weight	98 kg
Tool Centre Point TCP Max. Speed	250 mm/s
Endurance Load in XY Direction	± 1300 N
Endurance Load in Z Direction	± 1000 N
Endurance Torque in XY Direction	± 1300 N.m
Endurance Torque in Z Direction	± 300 N.m

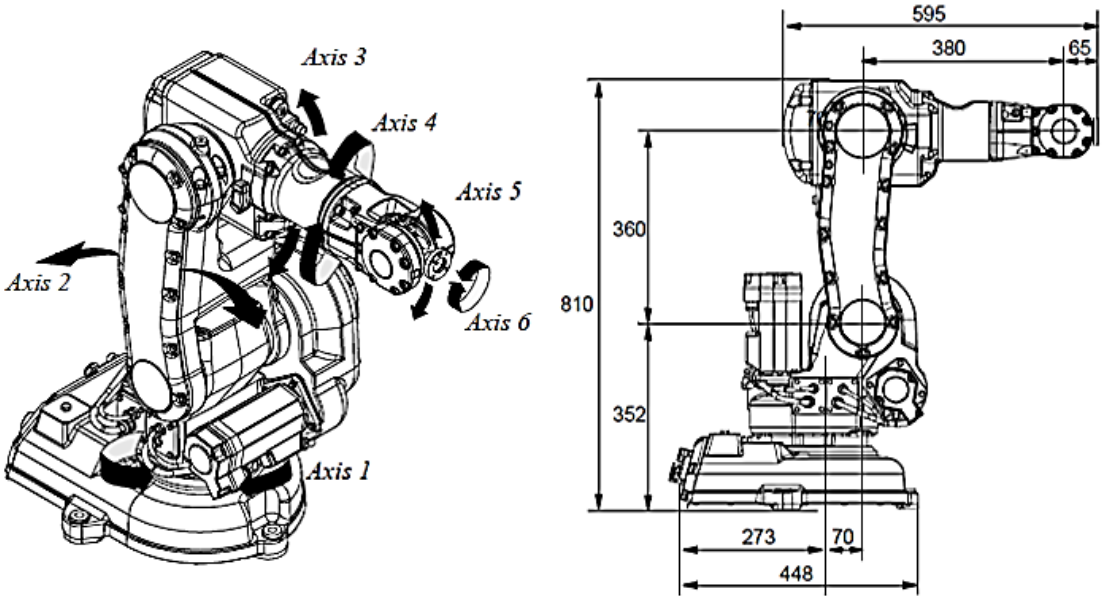

Figure 1. The ABB IRB 140 manipulator (ABB, 2000)

3.0 FORWARD KINEMATICS

To mathematically model a robot and hence determine the position and orientation of the end effector with respect to the base or any other point, it is necessary to assign a global coordinate frame to the base of the robot and a local reference frame at each joint. Then, the Denavit-Hartenberg analysis (DH) is presented to build the homogeneous transformation matrices between the robot joint axes (Craig, 2005) (Siciliano, Sciavicco, Villani, & Oriolo, 2010). These matrices are a function of four parameters resulted from a series of translations and rotations around different axes. The illustration of how frame {i} is related to the previous frame {i −1} and the description of the frame parameters are shown in figure 2 below.

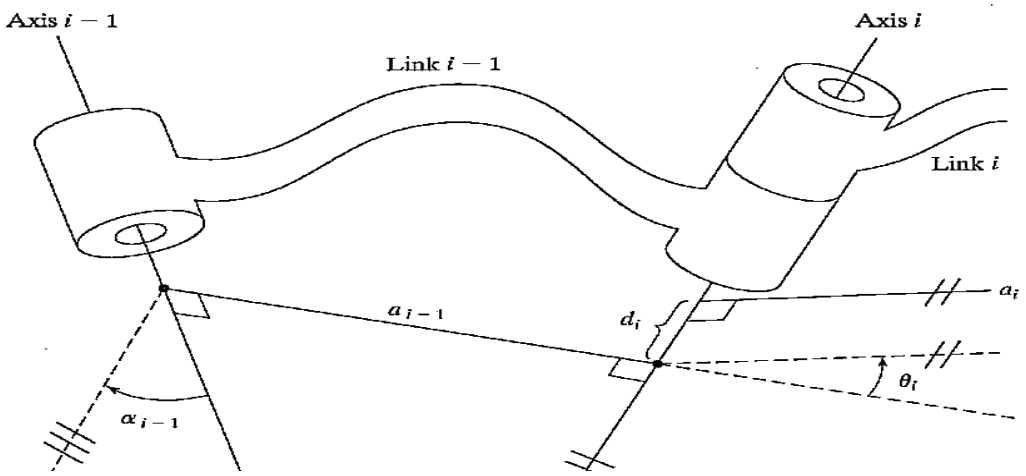

Figure 2. The description of frame {i} with respect to frame {i −1}(Craig, 2005)

These modified D-H parameters can be described as:

- α_{i-1}: Twist angle between the joint axes Z_i and Z_{i-1} measured about X_{i-1}.
- a_{i-1}: Distance between the two joint axes Z_i and Z_{i-1} measured along the common normal.
- θ_i: Joint angle between the joint axes X_i and X_{i-1} measured about Z_i.
- d_i: Link offset between the axes X_i and X_{i-1} measured along Z_i.

Thus, the four Transformations between the two axes can be defined as:

$$^{i-1}_{i}T = Rot(X_{i-1}, \alpha_{i-1}) \text{ x } Trans(X_{i-1}, a_{i-1}) \text{ x } Rot(Z_i, \theta_i) \text{ x } Trans(0,0,d_i)$$

After finishing the multiplication of these four transformations, the homogeneous transform can be obtained as:

$$^{i-1}_{i}T = \begin{pmatrix} c_{\theta_i} & -s_{\theta_i} & 0 & a_{i-1} \\ s_{\theta_i}c_{\alpha_{i-1}} & c_{\theta_i}c_{\alpha_{i-1}} & -s_{\alpha_{i-1}} & -d_i s_{\alpha_{i-1}} \\ s_{\theta_i}s_{\alpha_{i-1}} & c_{\theta_i}s_{\alpha_{i-1}} & c_{\alpha_{i-1}} & d_i c_{\alpha_{i-1}} \\ 0 & 0 & 0 & 1 \end{pmatrix} \quad (1.1)$$

The ABB IRB 140 frames assignment is shown below in figure 3.

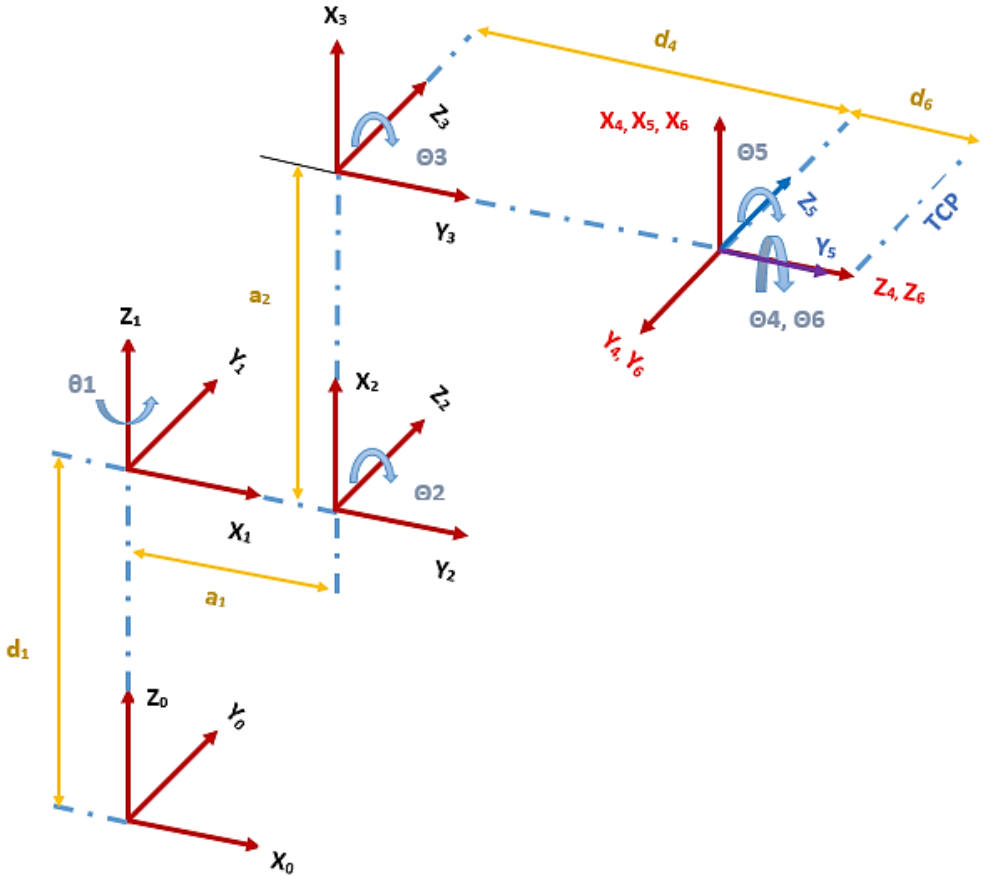

Figure 3. ABB IRB140 frames assignment

According to this particular frame assignment, the modified D-H parameters are defined in Table 2 below.

Table 2. The ABB IRB 140 D-H parameters

Axis (i)	α_{i-1}	a_{i-1}	d_i	θ_i
1	0	0	$d_1 = 352$	θ_1
2	-90	$a_1 = 70$	0	θ_2-90
3	0	$a_2 = 360$	0	θ_3
4	-90	0	$d_4 = 380$	θ_4
5	90	0	0	θ_5
6	-90	0	0	θ_6

For the simplicity of calculations and matrix product, it can be assumed that $S_2 = \sin(\theta_2\text{-}90)$, $C_2 = \cos(\theta_2\text{-}90)$. After achieving the D-H table, the individual transformation matrix for each link is achieved by substituting the link parameters into the general homogeneous transform derived in matrix (1.1) above.

$$ {}^{0}_{1}T = \begin{pmatrix} c_{\theta_1} & -s_{\theta_1} & 0 & a_0 \\ s_{\theta_1}c_{\alpha_0} & c_{\theta_i}c_{\alpha_{01}} & -s_{\alpha_0} & -d_1 s_{\alpha_0} \\ s_{\theta_1}s_{\alpha_0} & c_{\theta_1}s_{\alpha_0} & c_{\alpha_0} & d_1 c_{\alpha_0} \\ 0 & 0 & 0 & 1 \end{pmatrix} \qquad {}^{0}_{1}T = \begin{pmatrix} c_1 & -s_1 & 0 & 0 \\ s_1 & c_1 & 0 & 0 \\ 0 & 0 & 1 & d_1 \\ 0 & 0 & 0 & 1 \end{pmatrix} $$

$$ {}^{1}_{2}T = \begin{pmatrix} c_{\theta_2} & -s_{\theta_2} & 0 & a_1 \\ s_{\theta_2}c_{\alpha_1} & c_{\theta_2}c_{\alpha_1} & -s_{\alpha_1} & -d_2 s_{\alpha_1} \\ s_{\theta_2}s_{\alpha_1} & c_{\theta_2}s_{\alpha_1} & c_{\alpha_1} & d_2 c_{\alpha_1} \\ 0 & 0 & 0 & 1 \end{pmatrix} \qquad {}^{01}_{2}T = \begin{pmatrix} c_2 & -s_2 & 0 & a_1 \\ 0 & 0 & 1 & 0 \\ -s_2 & -c_2 & 0 & 0 \\ 0 & 0 & 0 & 1 \end{pmatrix} $$

$$ {}^{2}_{3}T = \begin{pmatrix} c_{\theta_3} & -s_{\theta_3} & 0 & a_2 \\ s_{\theta_3}c_{\alpha_2} & c_{\theta_3}c_{\alpha_2} & -s_{\alpha_2} & -d_3 s_{\alpha_2} \\ s_{\theta_3}s_{\alpha_2} & c_{\theta_3}s_{\alpha_2} & c_{\alpha_2} & d_3 c_{\alpha_2} \\ 0 & 0 & 0 & 1 \end{pmatrix} \qquad {}^{2}_{3}T = \begin{pmatrix} c_3 & -s_3 & 0 & a_2 \\ s_3 & c_3 & 0 & 0 \\ 0 & 0 & 1 & 0 \\ 0 & 0 & 0 & 1 \end{pmatrix} $$

$$ {}^{3}_{4}T = \begin{pmatrix} c_{\theta_4} & -s_{\theta_4} & 0 & a_3 \\ s_{\theta_4}c_{\alpha_3} & c_{\theta_4}c_{\alpha_3} & -s_{\alpha_3} & -d_4 s_{\alpha_3} \\ s_{\theta_4}s_{\alpha_3} & c_{\theta_4}s_{\alpha_3} & c_{\alpha_3} & d_4 c_{\alpha_3} \\ 0 & 0 & 0 & 1 \end{pmatrix} \qquad {}^{3}_{4}T = \begin{pmatrix} c_4 & -s_4 & 0 & 0 \\ 0 & 0 & 1 & d_4 \\ -s_4 & -c_4 & 0 & 0 \\ 0 & 0 & 0 & 1 \end{pmatrix} $$

$$ {}^{4}_{5}T = \begin{pmatrix} c_{\theta_5} & -s_{\theta_5} & 0 & a_4 \\ s_{\theta_5}c_{\alpha_4} & c_{\theta_5}c_{\alpha_4} & -s_{\alpha_4} & -d_5 s_{\alpha_4} \\ s_{\theta_5}s_{\alpha_4} & c_{\theta_5}s_{\alpha_4} & c_{\alpha_4} & d_5 c_{\alpha_4} \\ 0 & 0 & 0 & 1 \end{pmatrix} \qquad {}^{4}_{5}T = \begin{pmatrix} c_5 & -s_5 & 0 & 0 \\ 0 & 0 & -1 & 0 \\ s_5 & c_5 & 0 & 0 \\ 0 & 0 & 0 & 1 \end{pmatrix} $$

$$ {}^{5}_{6}T = \begin{pmatrix} c_{\theta_6} & -s_{\theta_6} & 0 & a_5 \\ s_{\theta_6}c_{\alpha_5} & c_{\theta_6}c_{\alpha_5} & -s_{\alpha_5} & -d_6 s_{\alpha_5} \\ s_{\theta_6}s_{\alpha_5} & c_{\theta_5}s_{\alpha_5} & c_{\alpha_5} & d_6 c_{\alpha_5} \\ 0 & 0 & 0 & 1 \end{pmatrix} \qquad {}^{5}_{6}T = \begin{pmatrix} c_6 & -s_6 & 0 & 0 \\ 0 & 0 & 1 & 0 \\ -s_6 & -c_6 & 0 & 0 \\ 0 & 0 & 0 & 1 \end{pmatrix} $$

Once the homogeneous transformation matrix of each link is obtained, forward kinematic chain can be applied to achieve the position and orientation of the robot end-effector with respect to the global reference frame (robot base).

$$ {}^{0}_{2}T = {}^{0}_{1}T \text{ X } {}^{1}_{2}T $$

$$ {}^{0}_{2}T = \begin{pmatrix} c_1 & -s_1 & 0 & 0 \\ s_1 & c_1 & 0 & 0 \\ 0 & 0 & 1 & d_1 \\ 0 & 0 & 0 & 1 \end{pmatrix} \text{X} \begin{pmatrix} c_2 & -s_2 & 0 & a_1 \\ 0 & 0 & 1 & 0 \\ -s_2 & -c_2 & 0 & 0 \\ 0 & 0 & 0 & 1 \end{pmatrix} = \begin{pmatrix} c_1c_2 & -c_1s_2 & -s_1 & c_1a_1 \\ s_1c_2 & -s_1s_2 & c_1 & s_1a_1 \\ -s_2 & -c_2 & 0 & d_1 \\ 0 & 0 & 0 & 1 \end{pmatrix} $$

$$ {}^{0}_{3}T = {}^{0}_{2}T \text{ X } {}^{2}_{3}T $$

$$ {}^{0}_{3}T = \begin{pmatrix} c_1c_2 & -c_1s_2 & -s_1 & c_1a_1 \\ s_1c_2 & -s_1s_2 & c_1 & s_1a_1 \\ -s_2 & -c_2 & 0 & d_1 \\ 0 & 0 & 0 & 1 \end{pmatrix} X \begin{pmatrix} c_3 & -s_3 & 0 & a_2 \\ s_3 & c_3 & 0 & 0 \\ 0 & 0 & 1 & 0 \\ 0 & 0 & 0 & 1 \end{pmatrix} $$

$$ {}^{0}_{3}T = \begin{pmatrix} c_1c_2c_3 - c_1s_2s_3 & -(c_1c_2s_3 + c_1s_2c_3) & -s_1 & c_1c_2a_2 + c_1a_1) \\ s_1c_2c_3 - s_1s_2s_3 & -(s_1c_2s_3 + s_1s_2c_3) & c_1 & s_1c_2a_2 + s_1a_1) \\ -(s_2c_3 + c_2s_3) & s_2s_3 - c_2c_3 & 0 & -s_2a_2 + d_1 \\ 0 & 0 & 0 & 1 \end{pmatrix} $$

$$ {}^{0}_{3}T = \begin{pmatrix} c_1c_{23} & -c_1s_{23} & -s_1 & c_1(c_2a_2 + a_1) \\ s_1c_{23} & -s_1s_{23} & c_1 & s_1(c_2a_2 + a_1) \\ -s_{23} & -c_{23} & 0 & -s_2a_2 + d_1 \\ 0 & 0 & 0 & 1 \end{pmatrix} $$

$$ {}^{4}_{6}T = {}^{4}_{5}T \text{ X } {}^{5}_{6}T $$

$$ {}^{4}_{6}T = \begin{pmatrix} c_5 & -s_5 & 0 & 0 \\ 0 & 0 & -1 & 0 \\ s_5 & c_5 & 0 & 0 \\ 0 & 0 & 0 & 1 \end{pmatrix} X \begin{pmatrix} c_6 & -s_6 & 0 & 0 \\ 0 & 0 & 1 & 0 \\ -s_6 & -c_6 & 0 & 0 \\ 0 & 0 & 0 & 1 \end{pmatrix} = \begin{pmatrix} c_5c_6 & -c_5s_6 & -s_5 & 0 \\ s_6 & c_6 & 0 & 0 \\ s_5\,c_6 & -s_5\,s_6 & c_5 & 0 \\ 0 & 0 & 0 & 1 \end{pmatrix} $$

$$ {}^{3}_{6}T = {}^{3}_{4}T \text{ X } {}^{4}_{6}T $$

$$ {}^{3}_{6}T = \begin{pmatrix} c_4 & -s_4 & 0 & 0 \\ 0 & 0 & 1 & d_4 \\ -s_4 & -c_4 & 0 & 0 \\ 0 & 0 & 0 & 1 \end{pmatrix} X \begin{pmatrix} c_5c_6 & -c_5s_6 & -s_5 & 0 \\ s_6 & c_6 & 0 & 0 \\ s_5\,c_6 & -s_5\,s_6 & c_5 & 0 \\ 0 & 0 & 0 & 1 \end{pmatrix} $$

$$ {}^{3}_{6}T = \begin{pmatrix} c_4c_5c_6 - s_4s_6 & -c_4c_5s_6 - s_4c_6 & -c_4s_5 & 0 \\ s_5\,c_6 & -s_5\,s_6 & c_5 & d_4 \\ -s_4c_5c_6 - c_4s_6 & s_4c_5s_6 - c_4c_6 & s_4s_5 & 0 \\ 0 & 0 & 0 & 1 \end{pmatrix} $$

$$ {}^{0}_{6}T = {}^{0}_{3}T \text{ X } {}^{3}_{6}T $$

$$ {}^{0}_{6}T = \begin{pmatrix} c_1c_{23} & -c_1s_{23} & -s_1 & c_1(c_2a_2 + a_1) \\ s_1c_{23} & -s_1s_{23} & c_1 & s_1(c_2a_2 + a_1) \\ -s_{23} & -c_{23} & 0 & -s_2a_2 + d_1 \\ 0 & 0 & 0 & 1 \end{pmatrix} X \begin{pmatrix} c_4c_5c_6 - s_4s_6 & -c_4c_5s_6 - s_4c_6 & -c_4s_5 & 0 \\ s_5\,c_6 & -s_5\,s_6 & c_5 & d_4 \\ -s_4c_5c_6 - c_4s_6 & s_4c_5s_6 - c_4c_6 & s_4s_5 & 0 \\ 0 & 0 & 0 & 1 \end{pmatrix} $$

$$ {}^{0}_{6}T = \begin{pmatrix} r11 & \text{r12} & \text{r13} & \text{x} \\ \text{r21} & \text{r22} & \text{r23} & \text{y} \\ \text{r31} & \text{r32} & \text{r33} & z \\ 0 & 0 & 0 & 1 \end{pmatrix} $$

$$ \text{r}_{11} = c_1c_{23}\,(c_4c_5c_6 - s_4s_6) - c_1s_{23}s_5\,c_6 + s_1(s_4c_5c_6 + c_4s_6) $$

$$ \text{r}_{12} = c_1c_{23}(-c_4c_5s_6 - s_4c_6) + c_1s_{23}s_5\,s_6 - s_1(s_4c_5s_6 - c_4c_6) $$

$$ \text{r}_{13} = -c_1c_{23}c_4s_5 - c_1s_{23}c_5 - s_1s_4s_5 $$

$r_{21} = s_1 c_{23} (c_4 c_5 c_6 - s_4 s_6) - s_1 s_{23} s_5 c_6 - c_1 (s_4 c_5 c_6 + c_4 s_6)$

$r_{22} = s_1 c_{23} (-c_4 c_5 s_6 - s_4 c_6) + s_1 s_{23} s_5 s_6 + c_1 (s_4 c_5 s_6 - c_4 c_6)$

$r_{23} = -s_1 c_{23} c_4 s_5 - s_1 s_{23} c_5 + c_1 s_4 s_5$

$r_{31} = -s_{23} (c_4 c_5 c_6 - s_4 s_6) - c_{23} s_5 c_6$

$r_{32} = -s_{23} (-c_4 c_5 s_6 - s_4 c_6) + c_{23} s_5 s_6$

$r_{33} = s_{23} c_4 s_5 - c_{23} c_5$

$x = -d_4 c_1 s_{23} + c_1 (c_2 a_2 + a_1)$

$y = -d_4 s_1 s_{23} + s_1 (c_2 a_2 + a_1)$

$z = -s_2 a_2 + d_1 - d_4 c_{23}$

It is also possible to find the position of the Tool Centre Point (TCP) with respect to the robot base. According to the robot frame assignment, it is simply a transition along the z axis of frame {6} by d_6 (distance from Joint 6 to the TCP). Therefore, the final position of the end effector with respect to the robot global reference frame can be expressed as:

$$P_{tcp} = {}^0_6T \; X \; P^6$$

$$P_{tcp} = \begin{pmatrix} r_{11} & r_{12} & r_{13} & x \\ r_{21} & r22 & r_{23} & y \\ r_{31} & r_{32} & r_{33} & z \\ 0 & 0 & 0 & 1 \end{pmatrix} X \begin{pmatrix} 0 \\ 0 \\ d_6 \\ 1 \end{pmatrix} = \begin{pmatrix} d_6 \, r_{13} + x \\ d_6 \, r_{23} + y \\ d_6 \, r_{33} + z \\ 1 \end{pmatrix}$$

4.0 FORWARD KINEMATIC VALIDATION

After finding the homogeneous transformation matrix (${}^0_6T$) that describes the end effector position and orientation with respect to the robot global reference frame, the position of the robot in space is expressed by the vector ${}^0P_{6ORG}$ which gives the values of x, y and z vectors as follow:

$x = -d_4 c_1 s_{23} + c_1 (c_2 a_2 + a_1)$

$y = -d_4 s_1 s_{23} + s_1 (c_2 a_2 + a_1)$

$z = -s_2 a_2 + d_1 - d_4 c_{23}$

Given: S_2 = Sin (θ_2-90), C_2 = Cos (θ_2-90),

d_1 = 352 mm, d_4 = 380 mm, a_1 = 70 mm

a_2 = 360 mm.

The above equations are programmed in Matlab and a set of eight positions, illustrated below in figure 4, were chosen randomly to validate the forward kinematic model. The joint angles of each position are entered manually by the user to obtain the x, y and z vectors as shown in table 3 below. It can be clearly seen that there is no y component corresponding to these particular positions because Θ_1 is always given to be zero. Then these joint angle values were entered through the robot operating software (Teach Pendant) in the lab. For each case, the actual robot position was similar to the x, y and z vector obtained from Matlab which proves the validity of the Matlab code.

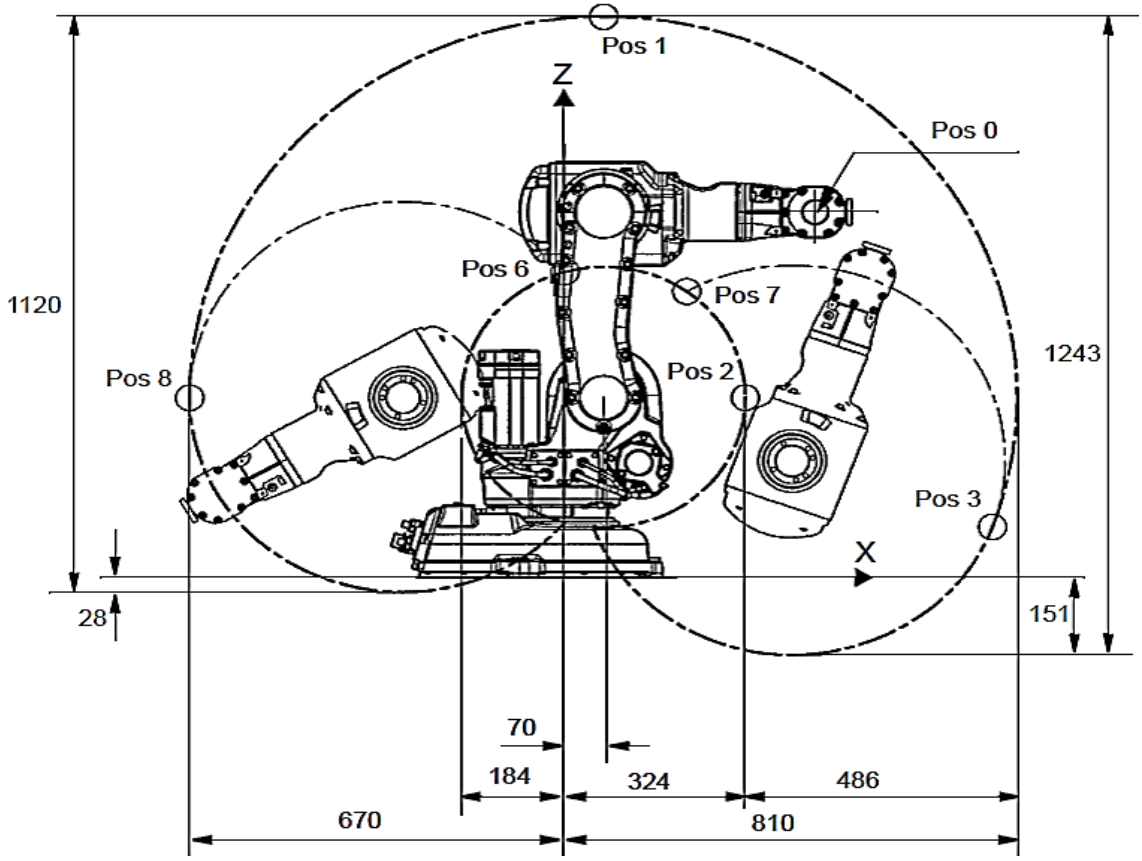

Figure 4. Set of robot's positions

Table 3. Matlab results of each position

Position	Joint angles	X vector	Y vector	Z vector
0	$\Theta_1 = 0, \Theta_2 = 0, \Theta_3 = 0$	450	0	712
1	$\Theta_1 = 0, \Theta_2 = 0, \Theta_3 = -90$	70	0	1092
2	$\Theta_1 = 0, \Theta_2 = 0, \Theta_3 = 50$	314	0	420.9
3	$\Theta_1 = 0, \Theta_2 = 110, \Theta_3 = -90$	765	0	98.9
6	$\Theta_1 = 0, \Theta_2 = -90, \Theta_3 = 50$	1.1	0	596
7	$\Theta_1 = 0, \Theta_2 = 110, \Theta_3 = -230$	218	0	558
8	$\Theta_1 = 0, \Theta_2 = -90, \Theta_3 = -90$	-670	0	352

5.0 INVERSE KINEMATICS

Inverse kinematics is used to calculate the joint angles required to achieve the desired position and orientation in the robot workspace. The configuration of the robot governs the selection of the solution method. Since three consecutive axes of the robot intersect at a common point, Pieper's solution can be applied which provides a huge simplification of the inverse kinematic problem. An algebraic solution can also be implemented through the use of the inverse trigonometric functions. However, Piper's solution is chosen because it can be easily coded in Matlab. Pieper's approach works on the principle of separating the position solution for Θ_1, Θ_2 and Θ_3 from the orientation solution to solve for Θ_4, Θ_5 and Θ_6 (Pires, 2007). In general, there are two methods of solution, the analytical and geometrical approaches. A geometrical approach is initially implemented to find the joint variables Θ_1, Θ_2 and Θ_3 that define the end effector position in space, while an analytical solution is applied to calculate the angles Θ_4, Θ_5 and Θ_6 which describe the end-effector orientation.

5.1 Geometrical Solution

According to the frame assignment shown in figure one, x and y components of frame {1} is the same as frame {0} because there is only a Z-directional offset between the two frames. Therefore, the projection of the wrist components on x-y plane of frame {0} has the same components on frame {1} (Carter, 2009; Vicente, 2007). In addition, since both link two and three are planar, the position vector in y direction changes with respect to θ_1 only. Thus, two possible solutions for θ_1 can be achieved by simply applying the arctangent function.

$$\theta_1 = atan2\,(Pytcp, Pxtcp), \tag{5.1}$$

$$\theta_1' = \Pi + \theta_1 \tag{5.2}$$

The solutions of θ_2 and θ_3 are obtained by considering the plane, shown in figure 5 below, formed by the second and third planar links with respect to the robot reference frame.

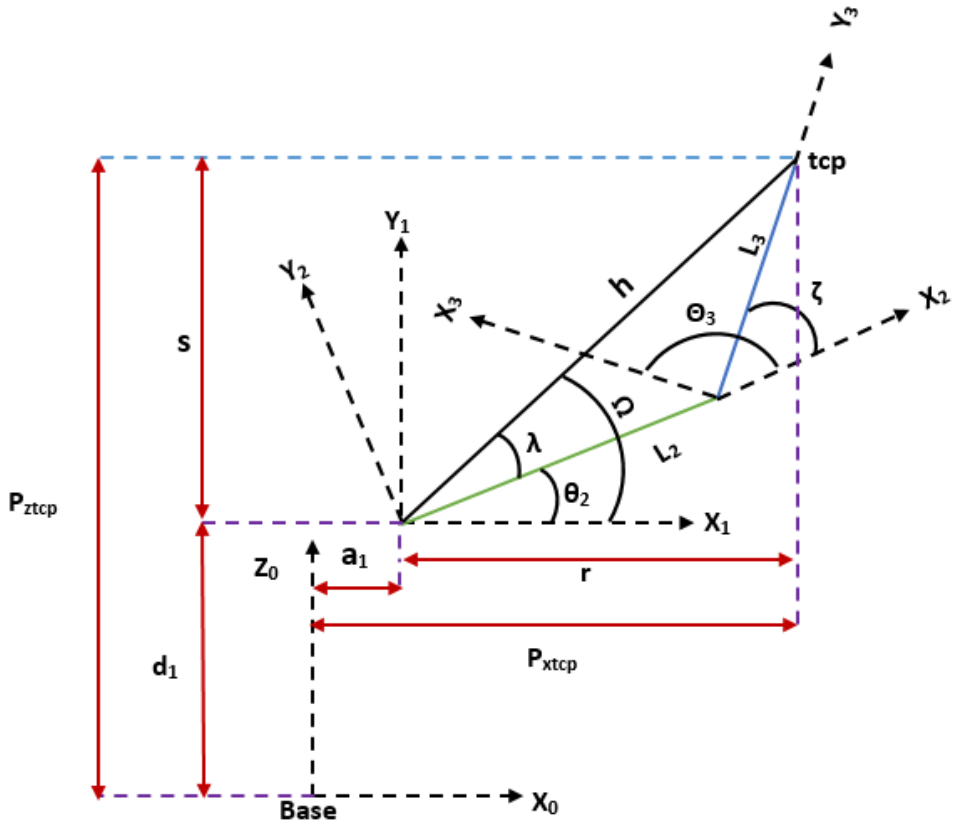

Figure 5. Projection of links two and three onto the x y plane

The cosine low is used to solve for θ3 as follow:

$$h^2 = L_2^2 + L_3^2 - 2\,x\,L_2\,x\,L_3\,x\,cos\,(180 - \zeta)$$

Since the position is given with respect to robot's Tool Center Point (TCP), L_3 should be equal to d_4+d_6, where d_6 is the distance from Joint 6 to the TCP. While,

$$L_2 = a_2\,, h^2 = s^2 + r^2\,, cos\,(180 - \zeta) = -cos\,(\zeta)$$

$$s^2 + r^2 = a_2^2 + (d_4 + d_6)^2 + 2\,x\,a_2\,x\,(d_4 + d_6)\,cos\,(\zeta)$$

$$Cos\,(\zeta) = \frac{s^2 + r^2 - a_2^2 - (d_4 + d_6)^2}{2\,x\,a_2\,x\,(d_4 + d_6)} \qquad (5.3)$$

Now, we should have the value of **(s)** and **(r)** in term of $\mathbf{P_{xtcp}}$, $\mathbf{P_{ytcp}}$, $\mathbf{P_{ztcp}}$ and $\boldsymbol{\theta_1}$.

$$S = (P_{ztcp} - d_1)$$

$$r = \pm\sqrt{(P_{xtcp} - a_1\,cos\,(\theta_1))^2 + (P_{ytcp} - a_1\,sin\,(\theta_1))^2}$$

Sub. (**s**) and (r) in (**5.3**) yield:

$$Cos\,(\zeta) = \frac{(P_{ztcp} - d_1)^2 + (P_{xtcp} - a_1\,Cos\,\theta_1)^2 + (P_{ytcp} - a_1\,Sin\,\theta_1)^2 - a_2^2 - (d_4 + d_6)^2}{2\,x\,a_2\,x\,(d_4 + d_6)}$$

$$Sin\,(\zeta) \;=\; \pm\sqrt{1 \;-\; Cos^2\,(\zeta)}$$

$$\zeta \;=\; atan2\,(Sin\,(\zeta), Cos\,(\zeta))$$

$$Finally, \theta 3 \;=\; -\,(90 \;+\; \zeta) \tag{5.4}$$

The negative sign in θ_3 indicates that the rotation occurred in the opposite direction. Likewise, we can follow the same procedure to solve for θ_2 using similar trigonometric relationships.

$$\theta_2 = \;\Omega - \lambda$$

$$\Omega \;=\; atan2\,(s, r)$$

$$\lambda \;=\; atan2\left((d_4 \;+\; d_6)\sin(\zeta), a_2 \;+ (d_4 \;+\; d_6)\cos(\zeta)\right)$$

$$\theta_2 = \;atan2\,(s, r) - atan2\left((d_4 \;+\; d_6)\sin(\zeta), a_2 \;+ (d_4 \;+\; d_6)\cos(\zeta)\right)$$

Substitute the values of (s) and (r) yield:

$$\theta_2 = \;atan2\left(\left(P_{ztcp} - d_1\right), \pm\sqrt{\left(P_{xtcp} - a_1\cos(\theta_1)\right)^2 + \left(P_{ytcp} - a_1\sin(\theta_1)\right)^2}\right) - atan2\,((d_4 \;+\; d_6)\,sin\,(\zeta), a_2 \;+\; (d_4 \;+\; d_6)\,cos\,(\zeta))$$

Again the rotation occurred in the opposite direction of the z axis as well as there are an initial rotation of 90^0 between axis 1 and axis 2. Thus, the final value of θ_2 is equal to:

$$\theta_2 = -\left((\Omega - \lambda) - 90\right) \tag{5.5}$$

It is important to say that any position within the robot workspace can be achieved with many orientations. Therefore, multiple solutions exist for the variables Θ_1, Θ_2 and Θ_3 due to the nature of trigonometric functions. In general, the problem of inverse kinematics may have eight solutions for the most six DOF manipulators (Nicolescu, Ilie, & Alexandru, 2015).

As noticed above, every solution step resulted in two values that will be used in the next step, and so on. For example, there are four solutions for ζ that resulted from two different values of Θ_1 [Θ_1 and $\Theta_{1'}$], this procedure gives four solutions for θ_3 [Θ_3 $\Theta_{3'}$ Θ_{3a} $\Theta_{3a'}$] and eight solutions for Θ_2 [Θ_2 $\Theta_{2'}$ Θ_{2a} $\Theta_{2a'}$ Θ_{2b} $\Theta_{2b'}$ Θ_{2c} $\Theta_{2a'}$], each set of solution corresponds to different robot configurations of elbow-up and elbow-down representations. These values are listed in table 4 below to illustrate all the possible solution set.

Table 4. Possible solution set

Solution	THETA1	THETA3	THETA2	Set
1	Θ_1	Θ_3	Θ_2	SET 1
2			$\Theta_{2'}$	
3		$\Theta_{3'}$	Θ_{2a}	SET 2
4			$\Theta_{2a'}$	
5	$\Theta_{1'}$	Θ_{3a}	Θ_{2b}	SET 3
6			$\Theta_{2b'}$	
7		$\Theta_{3a'}$	Θ_{2c}	SET 4
8			$\Theta_{2c'}$	

5.2 Analytical Solution

After solving the first inverse kinematic sub-problem which gives the required position of the end effector, the next step of the inverse kinematic solution will deal with the procedure of solving the orientation sub-problem to find the joint angles Θ_4, Θ_5 and Θ_6. This can be done using Z-Y-X Euler's formula. As the orientation of the tool frame with respect to the robot base frame is described in term of Z-Y-X Euler's rotation, this means that each rotation will take place about an axis whose location depends on the previous rotation (Craig, 2005). The Z-Y-X Euler's rotation is shown below in figure 6.

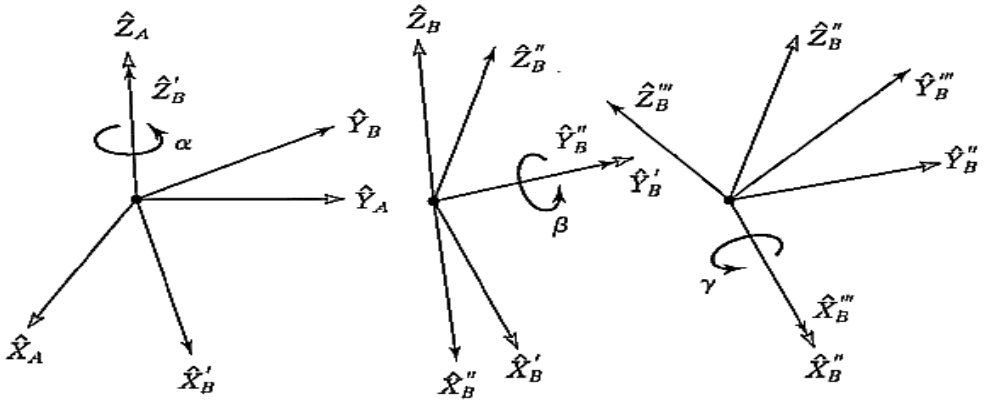

Figure 6. Z—Y—X Euler rotation

The final orientation matrix that results from these three consecutive rotations will be as follow:

$$^0_6R = \mathrm{R}_{z'y'x'} = \mathrm{R}_z\,(\alpha)\,\mathrm{R}_y\,(\beta)\,\mathrm{R}_x\,(\gamma)$$

$$^0_6R = \begin{pmatrix} c_\alpha & -s_\alpha & 0 \\ s_\alpha & c_\alpha & 0 \\ 0 & 0 & 1 \end{pmatrix} X \begin{pmatrix} c_\beta & 0 & s_\beta \\ 0 & 1 & 0 \\ -s_\beta & 0 & c_\beta \end{pmatrix} X \begin{pmatrix} 1 & 0 & 0 \\ 0 & c_\gamma & -s_\gamma \\ 0 & s_\gamma & c_\gamma \end{pmatrix}$$

$$^0_6R = \begin{pmatrix} c_\alpha c_\beta & c_\alpha s_\beta s_\gamma - s_\alpha c_\gamma & c_\alpha s_\beta c_\gamma + s_\alpha s_\gamma \\ s_\alpha c_\beta & s_\alpha s_\beta s_\gamma + c_\alpha c_\gamma & s_\alpha s_\beta c_\gamma - c_\alpha s_\gamma \\ -s_\beta & c_\beta s_\gamma & c_\beta c_\gamma \end{pmatrix}$$

Recall the forward kinematic equation,

$$ {}^{0}_{3}R = \begin{pmatrix} c_1c_{23} & -c_1s_{23} & -s_1 \\ s_1c_{23} & -s_1s_{23} & c_1 \\ -s_{23} & -c_{23} & 0 \end{pmatrix} $$

$$ {}^{3}_{6}R = ({}^{0}_{3}R)^{T} \; {}^{0}_{6}R $$

$$ {}^{3}_{6}R = \begin{pmatrix} c_1c_{23} & s_1c_{23} & -s_{23} \\ -c_1s_{23} & -s_1s_{23} & -c_{23} \\ -s_1 & c_1 & 0 \end{pmatrix} x \begin{pmatrix} c_\alpha c_\beta & c_\alpha s_\beta s_\gamma - s_\alpha c_\gamma & c_\alpha s_\beta c_\gamma + s_\alpha s_\gamma \\ s_\alpha c_\beta & s_\alpha s_\beta s_\gamma + c_\alpha c_\gamma & s_\alpha s_\beta c_\gamma - c_\alpha s_\gamma \\ -s_\beta & c_\beta s_\gamma & c_\beta c_\gamma \end{pmatrix} $$

$$ {}^{3}_{6}R = \begin{pmatrix} g_{11} & g_{12} & g_{13} \\ g_{21} & g_{22} & g_{23} \\ g_{31} & g_{32} & g_{33} \end{pmatrix} $$

However, it can be concluded that the last three intersected joints form a set of ZYZ Euler angles with respect to frame {3}. Therefore, these rotations can be expressed as:

$$ R_{z'y'z'} = {}^{3}_{6}R = R_z(\alpha)\, R_y(\beta)\, R_z(\gamma) $$

$$ {}^{3}_{6}R = \begin{pmatrix} c_\alpha & -s_\alpha & 0 \\ s_\alpha & c_\alpha & 0 \\ 0 & 0 & 1 \end{pmatrix} X \begin{pmatrix} c_\beta & 0 & s_\beta \\ 0 & 1 & 0 \\ -s_\beta & 0 & c_\beta \end{pmatrix} X \begin{pmatrix} c_\gamma & -s_\gamma & 0 \\ s_\gamma & c_\gamma & 0 \\ 0 & 0 & 1 \end{pmatrix} $$

$$ {}^{3}_{6}R = \begin{pmatrix} c_\alpha c_\beta c_\gamma - s_\alpha s_\gamma & -c_\alpha c_\beta s_\gamma - s_\alpha c_\gamma & c_\alpha s_\beta \\ s_\alpha c_\beta c_\gamma + c_\alpha s_\gamma & -s_\alpha c_\beta s_\gamma + c_\alpha c_\gamma & s_\alpha s_\beta \\ -s_\beta c_\gamma & s_\beta s_\gamma & c_\beta \end{pmatrix} $$

Where ${}^{3}_{6}R$ is given above as

$$ {}^{3}_{6}R = \begin{pmatrix} g_{11} & g_{12} & g_{13} \\ g_{21} & g_{22} & g_{23} \\ g_{31} & g_{32} & g_{33} \end{pmatrix} $$

It is possible now to use the ZYZ Euler's angles formula to obtain the solutions for Θ_4, Θ_5 and Θ_6 where

$$ \theta_5 = \beta = atan2\left(+\sqrt{g_{31}^2 + g_{32}^2}\,, g_{33}\right) \tag{5.6} $$

$$ \theta_4 = \alpha = atan2\left(\frac{g_{32}}{s_\beta}, \frac{-g_{31}}{s_\beta}\right) \tag{5.7} $$

$$ \theta_6 = \gamma = atan2\left(\frac{g_{23}}{s_\beta}, \frac{g_{13}}{s_\beta}\right) \tag{5.8} $$

For each of the eight solutions achieved from the geometric approach for Θ_1, Θ_2 and Θ_3, there is another flipped solution of Θ_4, Θ_5 and Θ_6 that can be obtained as:

$$\theta_5' = \beta' = atan2\left(-\sqrt{g_{31}^2 + g_{32}^2}\,, g_{33}\right), \quad \text{Or simply } \theta_5' = -\theta_5$$

$$\theta_4' = \alpha' = atan2\left(\frac{g_{32}}{s_{\beta'}}, \frac{-g_{31}}{s_{\beta'}}\right), \qquad \text{Or simply } \theta_4' = 180 + \theta_4$$

$$\theta_6' = \gamma' = atan2\left(\frac{g_{23}}{s_{\beta'}}, \frac{g_{13}}{s_{\beta'}}\right) \qquad \text{Or simply } \theta_6' = 180 + \theta_6$$

However, if β = 0 or 180, this means that the robot in a singular configuration where the joint axes 4 and 6 are parallel. This results in a similar motion of the last three intersection links of the robot manipulator.
Alternatively:

If $\beta = \theta_5 = 0$, the solution will be

$$\theta_4 = \alpha = 0$$

$$\theta_6 = \gamma = atan2\,(-g_{12}, g_{11})$$

And if $\beta = \theta_5 = 180$, the solution will be

$$\theta_4 = \alpha = 0$$

$$\theta_6 = \gamma = atan2\,(g_{12}, -g_{11})$$

6.0 INVERSE KINEMATIC VALIDATION

The home position of the robot in space is chosen to check the validity of the inverse kinematic solution. This position can be represented by a point (P_{tcp}) in the robot workspace. This point describes the position of the Tool Centre Point (TCP) with respect to the robot base frame. By applying the inverse kinematic equations derived above, a set of joint angles is achieved. However, some of these angles do not yield a valid solution which is simply due to the fact that not all the joints can be rotated by 360^0.

P_{tcp} (Home Position) $= [p_{xtcp}\ \ p_{ytcp}\ p_{ztcp}]^{\,T} = [515\ 0\ 712]^{\,T}$

After performing the calculations in MATLAB, four sets of solution were obtained as shown in table 5 below:

Table 5. All possible Inverse kinematics solutions

Θ_1	Θ_3	Θ_2	Set
0	-180	102	SET 1
		0	
	0	0	SET 2
		-102	
180	-153	93.7	SET 3
		-23	
	-27	23	SET 4
		-93.7	

However, because of the limitation on the joint angle range of movement, especially joints 2 and 3, some of these solutions are not valid. Nevertheless, they are shown above only to illustrate the calculation process. After that, these possible solutions are compared with the joint angle limits, listed below, and only valid solutions are presented in Matlab.

Table 6. ABB IRB 140 joint angle limits (ABB, 2000)

Joint Angle	MAX	MIN
Θ_1	180	-180
Θ_2	110	-90
Θ_3	50	-230
Θ_4	200	-200
Θ_5	115	-115
Θ_6	400	-400

After filtering all the possible solutions according to the joint angle limitation, only three valid solutions were achieved as shown in table 7.

Table 7. The valid inverse kinematics solutions

Θ_1	Θ_2	Θ_3	Set
0	0	0	1^{st}
180	-23	-153	2^{nd}
0	102	-180	3^{rd}

The three solutions, shown above, actually represent different robot configurations of the home position. These are default, elbow-up and elbow-down representations. The elbow-up configuration that corresponds to joint angles (180, -23, -153) is shown in figure 7 below, while figure 8 shows the elbow-down configuration that corresponds to joint angles (0, 102, 180). Finally, the set (0, 0, 0) represents the default home position. It is important to note that the position vector in Robot Studio is given for the TCP with respect to the robot global reference frame. Thus to match our solution with the simulation in Robot Studio, the inverse kinematics was solved with respect to the robot's TCP.

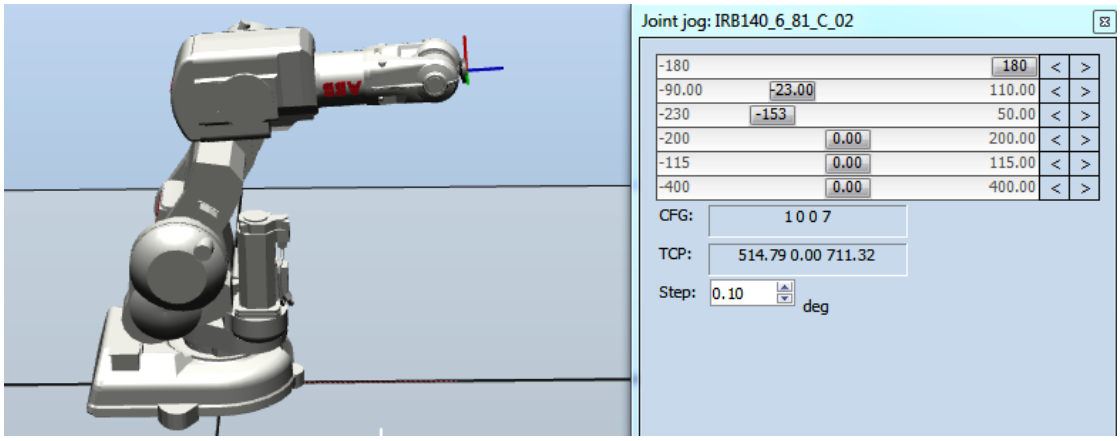

Figure 7. Elbow-up configuration

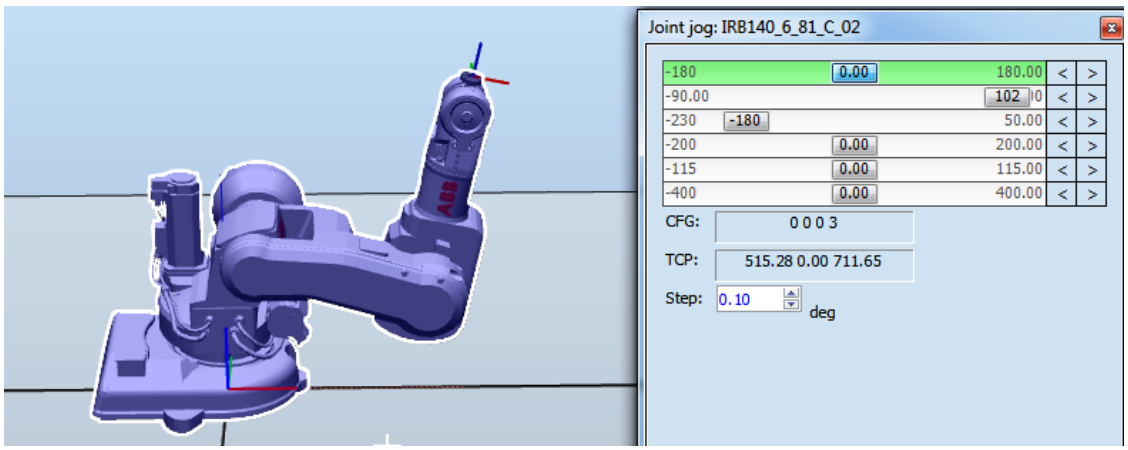

Figure 8. Elbow-down configuration

7.0 CONCLUSIONS

This work was undertaken to build the forward and inverse kinematic models of the ABB IRB 140 industrial manipulator. The Denavit-Hartenberg analysis (DH) is introduced to form the homogeneous transformation matrices. From the derived kinematic equations, it can be concluded that the position of the robot is given as a function of Θ_1, Θ_2 and Θ_3 only, while the three last intersection joint angles (Θ_4, Θ_5 and Θ_6) are used to give the desired orientation in space. The position vectors (x, y and z) obtained from the kinematic equations were matched with the actual robot position in the lab for the same joint angle input. Therefore, it can be declared that the kinematic derivation was carried out successfully. Two approaches have been presented to solve the inverse kinematic problem. Those were the geometrical and analytical approaches. Multiple solutions have been produced due to the nature of trigonometric functions. However, it has been shown that not all the solutions that resulted from the inverse kinematics were valid. This is basically due to the physical restrictions on the joint angle range of movement. A simulation of the manipulator in Robot Studio has been introduced to prove the validity of the inverse kinematic model. It is also used to validate the written Matlab code.

8.0 REFERENCES

ABB. (2000). IRB 140 M2000 Product Specification. Retrieved December 01, 2015 http://www.abb.com

Carter, T. J. (2009). *The Modeling of a Six Degree-of-freedom Industrial Robot for the Purpose of Efficient Path Planning.* The Pennsylvania State University.

Craig, J. J. (2005). *Introduction to robotics: mechanics and control*: Pearson/Prentice Hall Upper Saddle River, NJ, USA:.

Deshpande, V. A., & George, P. (2012). Analytical Solution for Inverse Kinematics of SCORBOT-ER-Vplus Robot. *International Journal of Emerging Technology and Advanced Engineering, 2*(3).

Feng, Y., Yao-nan, W., & Yi-min, Y. (2014). Inverse kinematics solution for robot manipulator based on neural network under joint subspace. *International Journal of Computers Communications & Control, 7*(3), 459-472.

Jazar, R. N. (2010). *Theory of applied robotics* (Vol. 1): Springer.

Khatamian, A. (2015). *Solving Kinematics Problems of a 6-DOF Robot Manipulator.* Paper presented at the Proceedings of the International Conference on Scientific Computing (CSC).

Mitra, A. K. (2012). Joint Motion-based Homogeneous Matrix Method for Forward Kinematic Analysis of Serial Mechanisms. *Int. J. Emerg. Technol. Adv. Eng, 2*, 111-122.

Neppalli, S., Csencsits, M. A., Jones, B. A., & Walker, I. D. (2009). Closed-form inverse kinematics for continuum manipulators. *Advanced Robotics, 23*(15), 2077-2091.

Nicolescu, A.-F., Ilie, F.-M., & Alexandru, T.-G. (2015). Forward and Inverse Kinematics Study of Industrial Robots Taking into Account Constructive and Functional Parameter's Moduling. *Proceedings in Manufacturing Systems, 10*(4), 157.

Paul, R. P. (1981). *Robot manipulators: mathematics, programming, and control: the computer control of robot manipulators*: Richard Paul.

Pires, J. N. (2007). *Industrial robots programming: building applications for the factories of the future*: Springer.

Samer Y, H. A., Moghavvemi M. (2009). *A New Geometrical Approach for the Inverse Kinematics of the Hyper Redundant Equal Length Links Planar Manipulators*.

Selig, J. (2013). *Geometrical methods in robotics*: Springer Science & Business Media.

Shahinpoor, M. (1987). *A robot engineering textbook*: Harper & Row Publishers, Inc.

Siciliano, B., Sciavicco, L., Villani, L., & Oriolo, G. (2010). *Robotics: modelling, planning and control*: Springer Science & Business Media.

Spong, M. W., Hutchinson, S., & Vidyasagar, M. (2006). *Robot modeling and control* (Vol. 3): Wiley New York.

Uicker, J. J., Pennock, G. R., & Shigley, J. E. (2011). *Theory of machines and mechanisms* (Vol. 1): Oxford University Press New York.

Vicente, D. B. (2007). *Modeling and Balancing of Spherical Pendulum Using a Parallel Kinematic Manipulator*.